JPET Fast Forward. Published on March 21, 2007 as DOI: 10.1124/jpet.107.120931
This article has not been copyedited and formatted. The final version may differ from this version.
JPET Fast Forward. Published on March 21, 2007 as DOI:10.1124/jpet.107.120931

Identification of I_{Kr} and its trafficking disruption induced by probucol in cultured neonatal rat cardiomyocytes

Jun Guo, Hamid Massaeli, Wentao Li, Jianmin Xu, Tao Luo, James Shaw, Lorrie A. Kirshenbaum and Shetuan Zhang

Institute of Cardiovascular Sciences, St. Boniface General Hospital Research Centre, Department of Physiology, Faculty of Medicine, University of Manitoba

JPET Fast Forward. Published on March 21, 2007 as DOI: 10.1124/jpet.107.120931
This article has not been copyedited and formatted. The final version may differ from this version.

Probucol disrupts I_{Kr} expression

Correspondence to: Shetuan Zhang, Ph D

Institute of Cardiovascular Sciences

St. Boniface General Hospital Research Centre and

Department of Physiology, Faculty of Medicine, University of Manitoba

351 Tache Avenue, Winnipeg, Manitoba

Canada R2H 2A6

Tel: (204) 235-3455

Fax: (204) 233-6755

E-mail: szhang@sbrc.ca

Total text pages: 22

Table: 1

Figures: 7

Total references: 32

Total words in abstract: 191

Total words in introduction: 376

Total words in discussion: 1055

Abbreviations:

hERG, human ether-a-go-go related gene; I_{Kr}, cardiac rapidly activating delayed rectifier K^+ current; LQTS, long QT syndrome; probucol, 4,4'-(isopropylidenedithio)-bis-(2,6-di-t-butylphenol); E-4031, 1-[2-(6-methyl-2-pyridyl)ethyl]-4-(methylsulfonyl-aminobenzoyl) piperidine; I-V, current-voltage.

JPET Fast Forward. Published on March 21, 2007 as DOI: 10.1124/jpet.107.120931
This article has not been copyedited and formatted. The final version may differ from this version.

ABSTRACT

The human ether-a-go-go-related gene (hERG) encodes a channel that conducts the rapidly activating delayed rectifier K^+ current (I_{Kr}) which is important for cardiac repolarization. Mutations in hERG reduce I_{Kr} and cause congenital long QT syndrome (LQTS). More frequently, common medications can reduce I_{Kr} and cause LQTS as a side effect. Protein trafficking abnormalities are responsible for most hERG mutation-related LQTS and are recently recognized as a mechanism for drug-induced LQTS. While hERG trafficking has been studied in recombinant expression systems, there has been no reported study on cardiac I_{Kr} trafficking at the protein level. In the present study, we identified that I_{Kr} is present in cultured neonatal rat ventricular myocytes, and can be robustly recorded using Cs^+ as the charge carrier. We further discovered that probucol, a cholesterol-lowering drug that induces LQTS, disrupted I_{Kr} trafficking and prolonged the cardiac action potential duration. Probucol did not directly block I_{Kr}. Probucol also disrupted hERG trafficking and did not block hERG channels expressed in HEK 293 cells. We conclude that probucol induces LQTS by disrupting ERG trafficking, and that primary culture of neonatal rat cardiomyocytes represents a useful system for studying native I_{Kr} trafficking.

JPET Fast Forward. Published on March 21, 2007 as DOI: 10.1124/jpet.107.120931
This article has not been copyedited and formatted. The final version may differ from this version.

INTRODUCTION

The human ether-a-go-go-related gene (hERG) encodes a K^+ channel that conducts the rapidly activating delayed rectifier K^+ current (I_{Kr}) (Sanguinetti *et al.*, 1995; Trudeau *et al.*, 1995). Reduction in I_{Kr} can cause long QT syndrome (LQTS), a cardiac repolarization disorder that can lead to life-threatening arrhythmias, Torsades de Pointes, and sudden cardiac death (Keating and Sanguinetti, 2001). Whereas direct blockade of hERG channels by various compounds represents a common mechanism for drug-induced LQTS (Sanguinetti and Tristani-Firouzi, 2006), recent evidence indicates that drug-disrupted hERG trafficking represents another mechanism for drug-induced LQTS (Ficker et al., 2004; Kuryshev et al., 2005; Cordes et al., 2005; Rajamani et al., 2006). Probucol is a cholesterol-lowering drug which has been known for many years to cause LQTS and Torsades de Pointes arrhythmia in humans and experimental animals (Elharrar *et al.*, 1979; McCaughan, 1982; Jones *et al.*, 1984). In a previous report studying wild type (WT) and M124T mutant hERG channels expressed in Xenopus oocyte, Hayashi *et al.* showed that probucol (30 μM) did not affect the hERG current amplitude during depolarization steps, but decreased the tail currents due to a ~10 mV shift of activation curve to the depolarized direction (Hayashi *et al.*, 2004). It is unknown whether probucol causes similar effects on hERG channels expressed in mammalian cell lines.

Presently, much of the available data of I_{Kr} are obtained in hERG channels expressed in mammalian cell lines or Xenopus oocyte. Since the pore-forming subunits of K^+ channels incorporate modulatory (β) subunits (Abbott *et al.*, 1999), kinase anchoring proteins (Gong *et al.*, 1999), cytoskeletal elements and other proteins, it is necessary to directly study native I_{Kr}. However, due to difficulties such as isolating I_{Kr} from other cardiac K^+ currents there has been no reported study demonstrating native I_{Kr} trafficking at the protein level. In the present study, we identified I_{Kr} in

JPET Fast Forward. Published on March 21, 2007 as DOI: 10.1124/jpet.107.120931
This article has not been copyedited and formatted. The final version may differ from this version.

neonatal rat ventricular myocytes, which can be recorded at a sufficiently robust level using Cs^+ as the charge carrier in whole-cell clamp recordings. Using this native I_{Kr} model, we found that clinically relevant concentrations of probucol reduce I_{Kr} and prolong the cardiac action potential duration via reducing I_{Kr} membrane expression but not via channel blockade. Our study demonstrated that primary culture of neonatal rat cardiomyocytes represents an effective model system for studying cardiac I_{Kr} trafficking.

JPET Fast Forward. Published on March 21, 2007 as DOI: 10.1124/jpet.107.120931
This article has not been copyedited and formatted. The final version may differ from this version.

MATERIALS AND METHODS

Neonatal Rat Ventricular Myocyte Isolation

Experimental protocols used for animal studies were approved by University of Manitoba Animal Care Committee. Single ventricular myocytes were isolated from 1 to 2-day old Sprague-Dawley rats of either sex by enzymatic dissociation as previously described (Baetz *et al.*, 2005). Cells were cultured in DMEM/F12 medium (Invitrogen) with 10% fetal bovine serum. Cardiomyocytes grown on glass coverslips for the electrophysiology study had a “spindle” morphology with a mean capacitance of 13.8 ± 1.3 pf (n = 33).

Molecular Biology

The hERG-HEK cells (HEK 293 cells stably expressing hERG channels) were a gift from Dr. Craig January (University of Wisconsin-Madison) (Zhou *et al.*, 1998b). In this cell line, hERG cDNA (Trudeau *et al.*, 1995) was subcloned into *Bam*HI/*Eco*RI sites of the pcDNA3 vector (Invitrogen, Carlsbad, CA). hERG cDNA in pcDNA3 was obtained from Dr. Gail Robertson (University of Wisconsin-Madison) (Trudeau *et al.*, 1995). For immunofluorescence staining of the cell surface hERG channels, a HA-epitope tag of the sequence ^{436}TEEGPPAT**NSEHYPYDVPDYAVTFE**ECGY (bold: insertion; underlined: HA epitope) was inserted into the extracellularly located S1-S2 loop of hERG channels to generate hERG-HAex via PCR using overlap extension method as previously described (Zhang, 2006). The hERG-HAex was transfected to HEK 293 cells and a stable hERG-HAex cell line (hERG-HAex-HEK) was created using G418. The insertion of HA did not change the electrophysiological and trafficking properties of hERG channels (data not shown), consistent with the results from Ficker *et al.* (Ficker *et al.*, 2003).

JPET Fast Forward. Published on March 21, 2007 as DOI: 10.1124/jpet.107.120931
This article has not been copyedited and formatted. The final version may differ from this version.

Patch Clamp Recording Method

Whole cell patch clamp method was used (Hamill *et al.*, 1981). The compositions of pipette and bath solutions for recording various currents are summarized in Table 1. Probucol was dissolved in ethanol to make 10-30 mM stock solutions. Procedures of whole-cell patch clamp method and Cs^+-carried I_{Kr} recording were performed as previously described (Zhang, 2006). Patch clamp experiments were performed at room temperature (23 ± 1°C).

Western Blot Analysis

Membrane proteins from hERG-HEK cells were isolated using Mem-PER Eukaryotic Membrane Protein Extraction Reagent Kit (Pierce Biotechnology, Rockford, IL). Membrane protein (10 µg/lane) we re separated on 7% SDS-PAGE gels and transferred onto nitrocellulose membranes. The membranes were blocked using Western Breeze Blocking Reagent (Invitrogen) and incubated with primary goat anti-hERG antibody (C-20, Santa Cruz Biotechnology, CA) and secondary anti-goat Western Breeze Chromogenic Detection Kit (Invitrogen). For cleavage of cell surface proteins, cells were washed with Phosphate Buffered Saline (PBS) and treated with 200 µg/ml proteinase K (Sigma) in a physiological buffer (10 mM HEPES, 150 mM NaCl and 2 mM $CaCl_2$, pH 7.4) at 37 °C. The reaction was terminated by adding ice-cold PBS containing 6 mM phenylmethylsulfonyl fluoride and 25 mM EDTA, and membrane protein was then extracted for Western blot analysis.

To extract membrane proteins from neonatal rat cardiac myocytes, cells from 100 mm plates were rinsed with ice-cold PBS and scraped off into a 1 ml solution containing 200 mM NaCl, 33 mM NaF, 10 mM EDTA, 50 mM HEPES (pH 7.4 with NaOH) plus a protease inhibitor cocktail. The cells were homogenized and spun at 500 × g for 10 min. The membrane fractions were pelleted

JPET Fast Forward. Published on March 21, 2007 as DOI: 10.1124/jpet.107.120931
This article has not been copyedited and formatted. The final version may differ from this version.

from the low-speed supernatants by centrifugation at 100,000 rpm for 1 h at 4°C, and re-suspended in 50 mM Tris-HCl, 15 mM mercaptoethanol, and 1% SDS. The membrane proteins (50 µg/sample) were boiled in sample buffer and electrophoresed on a 7% polyacrylamide SDS gel. The membrane proteins were then electrophoretically transferred onto nitrocellulose membrane using a trans-blot system (Bio-Rad). After transfer, the filters were blocked with 5% nonfat dry milk and 0.1% Tween 20 in Tris-Buffered Saline (TBS) for 1 h. The filters were then incubated with goat polyclonal anti-hERG (C-20) antibody at a 1:200 dilution at 4°C overnight. The filters were then washed with Tris-Buffered Saline Tween-20 (TBST) solution and incubated with horseradish peroxidase-conjugated donkey anti-goat immunoglobulin diluted 1:60000 in TBST for 1 h at room temperature. After washing with TBST, bound antibodies were detected with an ECL detection kit.

Isolation of Cell Surface Protein with Biotinylating Reagent

A Cell Surface Protein Isolation Kit (Pierce) was used to study the effects of probucol on the cell surface hERG expression. hERG-HEK cells were prepared in 100 mm cell culture plates at 90% confluence. The cells treated with vehicle control (0.3% ethanol) or 100 µM probucol for 48 h were washed twice with ice-cold PBS and labeled with 10 ml of membrane-impermeant biotinylating reagent, Sulfo-NHS-SS-biotin for 30 min at 4°C. The quenching solution (0.5 ml) was then added to quench the reaction. Cells were then lysed with 0.5 ml of lysis buffer with a protease inhibitor cocktail. After centrifugation at 10,000 × g for 2 min at 4°C, the cell lysate was then precipitated with Immobilized NeutrAvidin™ Gel (agarose beads). The bound proteins were released by incubating the resin with SDS-PAGE sample buffer (62.5 mM Tris-HCl, PH 6.8, 1% SDS, 10% glycerol) containing 50 mM DTT. The biotinated cell surface protein was subjected to 7% SDS-polyacrylamide gel electrophoresis and analyzed using primary goat anti-hERG antibody (C-20,

JPET Fast Forward. Published on March 21, 2007 as DOI: 10.1124/jpet.107.120931
This article has not been copyedited and formatted. The final version may differ from this version.

Santa Cruz) and horseradish peroxidase-conjugated donkey anti-goat secondary antibody, and detected with an ECL detection kit.

hERG siRNA Transfection

To inhibit ERG mRNA, cultured neonatal rat cardiomyocytes and hERG-HEK cells were transfected with hERG siRNA (Santa Cruz) or mouse ERG siRNA (of which one strand targets identical stretches in nucleotide sequence of rat ERG, Santa Cruz) using Lipofectamine 2000 (Invitrogen, Burlington, Ontario) according to the protocols recommended by the suppliers. Scrambled siRNA (Santa Cruz) was used as a negative control. Experiments were performed 48 h after transfection. For electrophysiology studies, pIRES2-EGFP (Clontech, Palo Alto, CA) was included in the transfection reagent during ERG siRNA transfection, and fluorescent-positive cells were selected for I_{Kr} or hERG current recordings.

Immunocytochemistry

For immunofluorescent studies, hERG HAex-HEK cells were plated on coverslips for growth under control conditions and in the presence of probucol. Cells were fixed under a non-permeabilized condition with 4% paraformaldehyde (Sigma) for 10 min at room temperature. After washing three times with PBS, cells were blocked with PBS containing 5% bovine serum albumin and 2% skim milk. The cells were immunostained with a rabbit anti-HA primary antibody (Anti-HA, 1:500, Sigma) and a green-fluorescent Alexa Fluor 488-conjugated donkey anti-rabbit IgG secondary antibody (1:250, Invitrogen). Cells were visualized using a Nikon TE2000-U research microscope (Nikon, Canada).

JPET Fast Forward. Published on March 21, 2007 as DOI: 10.1124/jpet.107.120931
This article has not been copyedited and formatted. The final version may differ from this version.

Data are expressed as the mean ± the standard error of the mean (S.E.). A one-way ANOVA or Student's *t*-test was used to determine the significance of differences between control and test groups. A *P*-value of 0.05 or less was considered significant.

JPET Fast Forward. Published on March 21, 2007 as DOI: 10.1124/jpet.107.120931
This article has not been copyedited and formatted. The final version may differ from this version.

RESULTS

Identification of I_{Kr} in Neonatal Rat Ventricular Myocytes

Figure 1Aa illustrates K^+ currents recorded from a neonatal rat ventricular myocyte. The pipette solution contained 135 mM K^+ and the bath solution contained 5 mM K^+ (Table 1). From a holding potential of −60 mV the cell was depolarized to voltages between −50 and 50 mV in 10 mV increments. Upon depolarizing steps, 68% (26 out of 38) of cells displayed the transient outward current (I_{to}). Notably, 95% (36 out of 38) of cells displayed the delayed outward K^+ current that was accompanied by the slow-decay tail current upon voltage returns to −50 mV. Both delayed outward currents and tail currents were completely abolished by the methanesulfonanilide compound E-4031 (1 µM), a specific blocker of I_{Kr} (Fig. 1Ab). The E-4031-sensitive currents were obtained by subtracting the whole cell current after application of 1 µM E-4031 from that before application of E-4031 in the same cell. Figure 1Ac shows the E-4031-sensitive currents. Figure 1B shows the averaged current-voltage (I-V) relationships of the E-4031-sensitive currents obtained from 4 cells. The currents at the end of depolarizing steps displayed the inward rectification which is characteristic to I_{Kr} (Fig. 1B, ■). The tail currents were plotted against the depolarizing voltages and the data were fitted to the Boltzmann equation (Fig. 1B, ●). The half-activation voltage ($V_{1/2}$) was –6.2 ± 1.7 mV and the slope factor was 6.9 ± 1.5 mV (n = 4 cells).

E-4031 sensitive I_{Kr} is small, and its recording represents a tedious task. Moreover, any alterations of K^+ currents during recordings before and after E-4031 will make the subtraction inaccurate. To address this difficulty, we recorded the pure I_{Kr} in neonatal rat ventricular myocytes using isotonic Cs^+ solutions (135 mM Cs^+_i/135 mM Cs^+_o, Table 1). We recently showed that hERG and I_{Kr} channels display unique Cs^+ permeability (Zhang, 2006). Since Cs^+ blocks most cardiac K^+ channels, Cs^+-carried I_{Kr} represents a simple and reliable way to directly record I_{Kr} (Zhang, 2006).

Figure 1C shows a family of Cs^+ currents obtained from a single cardiomyocyte. From a holding potential of –80 mV, depolarizations in 10 mV increments to voltages between –70 and +70 mV for 1 s were applied to evoke currents. Depolarizing steps to voltages more positive than 0 mV induced outward currents that inactivated in a voltage-dependent manner. The following tail currents at –80 mV displayed an initial rising phase, which is usually described as a "hook", reflecting the rapid recovery of inactivated channels to the open state prior to deactivation, and is unique to I_{Kr}. Figure 1D shows the I-V relationships of peak currents (▲), and currents at the end of 1 s depolarizing steps (■). Figure 1E shows the tail current activation curve. The $V_{1/2}$ and slope factor (k) were –41.7 ± 3.4 and 5.8 ± 0.3 mV, respectively (n = 8 cells). The relatively negative $V_{1/2}$ was due to the absence of Ca^{2+} in the bath solution (Zhang, 2006). The average Cs^+ tail current density measured at –80 mV following full channel activation was 17.9 ± 3.3 pA/pF (n = 8 cells).

To further demonstrate that the Cs^+ current recorded from neonatal rat cardiomyocytes indeed represents the Cs^+-carried I_{Kr}, the voltage-dependent inactivation and recovery from inactivation, which are unique to I_{Kr}, were analyzed. Figure 2A shows the voltage dependence of inactivation of Cs^+-carried I_{Kr}. The membrane was initially depolarized to +60 mV for 500 ms to inactivate the channels. A 20 ms repolarizing step to –100 mV was applied to recover inactivated channels to the open state. Prior to deactivation, the membrane was depolarized to various voltages to induce channel inactivation (current decay) which was fitted to a single exponential function to obtain the inactivation time constant (τ_{inact}). Figure 2B shows the recovery from inactivation of the Cs^+-carried I_{Kr}. The channels were activated and inactivated by a 500 ms depolarizing pulse to +60 mV. Repolarizing voltages between –10 and –120 mV were applied to record tail currents. The time constants of recovery from inactivation (τ_{rec}) were obtained by fitting the rising phase of the tail

JPET Fast Forward. Published on March 21, 2007 as DOI: 10.1124/jpet.107.120931
This article has not been copyedited and formatted. The final version may differ from this version.

currents to a single exponential function at different voltages (Sanguinetti *et al.*, 1995). Values of τ_{inact} (▼, n = 6) and τ_{rec} (▲, n = 6) are summarized and plotted against the membrane voltages (Fig. 2C). It has been known that extracellular Cs^+ slows hERG and I_{Kr} inactivation (Zhang, 2006). Consistent with the Cs^+ current in neonatal rat ventricular myocytes being Cs^+-carried I_{Kr}, the Cs^+ current inactivation was slowed by Cs^+ (Fig. 2D-F). As well, the Cs^+ current was entirely sensitive to hERG/I_{Kr} blocker E-4031 with IC_{50} and Hill coefficient of 2.0 ± 0.4 μM and 1.2, respectively (Fig. 2G-I, n = 4).

Western blot analysis was used to identify I_{Kr} proteins in neonatal ventricular myocytes. As shown in Fig. 3A, the hERG C-terminus antibody (HERG C-20, Santa Cruz) consistently identified four bands at sizes of approximately 150, 130, 95 and 85 kDa (n = 5 different myocyte isolations). The two higher molecular mass bands (150 and 130 kDa) are similar in size with mature glycosylated and immature core-glycosylated rat ERG1a (Jones *et al.*, 2004). The two lower molecular mass bands are consistent in size with mature glycosylated and core-glycosylated rat ERG1b (Jones *et al.*, 2004). To confirm that the 150 and 95 kDa bands represent the plasma membrane forms of ERG, we cleaved cell surface proteins by treating neonatal cardiomyocytes with proteinase K. As shown in Fig. 3A, proteinase K treatment significantly reduced the 150 and 95 kDa bands and this was accompanied by the appearance of an additional 60-70 kDa band. This treatment did not affect the 130 or 85 kDa bands of the ERG proteins (n = 5). Figure 3B shows Western blot of hERG proteins extracted from hERG-HEK cells (hERG1a). As reported previously (Zhou *et al.*, 1998b; Kuryshev *et al.*, 2005), hERG displayed two bands with molecular weights of 155 and 135 kDa (Fig. 3B), representing the mature fully glycosylated membrane form (155 kDa) and the immature core-glycosylated ER form (135 kDa) (Zhou *et al.*, 1998b; Zhou *et al.*, 1998a; Ficker *et al.*, 2004;

JPET Fast Forward. Published on March 21, 2007 as DOI: 10.1124/jpet.107.120931
This article has not been copyedited and formatted. The final version may differ from this version.

Kuryshev *et al.*, 2005). The 155 kDa hERG protein is localized on the plasma membrane since it was cleaved by proteinase K treatment (Fig. 3B, n = 3).

The siRNA of hERG were used to interfere with ERG mRNA and hERG/I_{Kr} expression. The siRNA of hERG (Santa Cruz; mRNA Accession #: NM_000238) has a sense strand sequence CCAUCAAGGACAAGUAUGU which targets the nucleotides of S5 side of the P-loop of hERG (between 1817 and 1835). This sequence also targets the nucleotides between 1823 and 1841 of rat ERG with one nucleotide difference. Scrambled siRNA (Santa Cruz) was used as control. Transfection with hERG siRNA reduced 4 bands of rat ERG proteins with a similar extent with 130 kDa band being reduced by 75 ± 4 % in neonatal rat cardiomyocytes (Fig. 3C, n = 4). Transfection with hERG siRNA reduced both hERG 135 and 155 kDa bands with 135 kDa band being reduced by 83 ± 7 % in hERG-HEK cells (Fig. 3D, n = 3). For electrophysiology studies, hERG siRNA or scrambled siRNA was transfected along with GFP (pIRES2-EGFP, Clontech, Palo Alto, CA). The I_{Kr} Cs^+ current in neonatal cardiomyocytes and the hERG K^+ current in hERG-HEK cells were recorded in GFP positive cells. Compared to I_{Kr} or hERG currents recorded in cells transfected with control siRNA, I_{Kr} was reduced by 81 ± 9 % (n = 10 for control siRNA; n = 16 for hERG siRNA; p<0.01), and hERG current was reduced by 87 ± 2 % (n = 8, for control siRNA; n = 9 for hERG siRNA; p<0.01) in cells transfected with hERG siRNA (Fig. 3E&F). Furthermore, in neonatal rat cardiomyocytes, transfection of a mixture of 3 mouse ERG siRNA which are highly homologous to rat ERG (strand-A 100% targeting region 987-1005 of rat nucleotide sequence, accession # NM_053949.1, strand-B targeting 1469-1487 with one nucleotide difference, and strand-C targeting 2635-2653 with one nucleotide difference) reduced I_{Kr} by 83 ± 6 % (n = 8 for control siRNA; n = 9 for mouse ERG siRNA; p<0.01).

Probucol Reduces ERG Expression

JPET Fast Forward. Published on March 21, 2007 as DOI: 10.1124/jpet.107.120931
This article has not been copyedited and formatted. The final version may differ from this version.

Our results indicate that Cs^+-carried I_{Kr} in neonatal rat cardiomyocytes can be recorded at a level that is large enough and sufficiently robust to evaluate I_{Kr} alterations. Next, we investigated the mechanisms of probucol-induced LQTS by studying the effects of probucol on I_{Kr} Cs^+ current in neonatal rat ventricular myocytes. Probucol is a cholesterol-lowering drug that causes LQTS in humans (Elharrar et al., 1979; McCaughan, 1982; Jones et al., 1984; Hayashi et al., 2004). We found that acute application of 100 μM probucol had no effect on I_{Kr} (Fig. 4A, n = 5). Figure 4A shows Cs^+-carried I_{Kr} recorded from a cardiomyocyte before and after acute application of 100 μM probucol. The tail current-activation voltage relationships were shown at the bottom of Fig. 4A. The $V_{1/2}$ and slope factor were −38.5 ± 1.6 and 6.7 ± 0.5 mV, respectively, in the absence of probucol (n = 5 cells). They were −39.5 ± 1.7 and 6.6 ± 0.6 mV in the presence of probucol (n = 5 cells, $p>0.05$). Thus, probucol had no acute effect on I_{Kr} in neonatal cardiomyocytes. However, chronic treatment of cardiomyocytes with probucol substantially reduced I_{Kr}. Figure 4B shows Cs^+-carried I_{Kr} from cardiomyocytes cultured in the absence (0.3% ethanol vehicle) or presence of 100 μM probucol for 48 h. The tail current-activation voltage relationships were summarized from 5 cells in the absence of probucol and from 7 cells in the presence of 30 μM probucol. The $V_{1/2}$ and slope factor were −42.2 ± 3.3 and 6.1 ± 0.7 mV, respectively, in control. They were −39.1 ± 2.9 and 6.6 ± 0.5 mV in probucol-treated cells ($p>0.05$). Thus while chronic application of probucol reduced I_{Kr} amplitude, it did not affect the voltage dependence of activation of I_{Kr}. Probucol-induced I_{Kr} reduction was concentration dependent. The bottom of Figure 4B shows the summarized I_{Kr} tail current amplitudes from myocytes treated with various concentrations of probucol for 48 h (n = 5-12 for each concentration). The IC_{50} and Hill coefficient were 20.6 ± 1.6 μM and 0.9 ± 0.1, respectively.

JPET Fast Forward. Published on March 21, 2007 as DOI: 10.1124/jpet.107.120931
This article has not been copyedited and formatted. The final version may differ from this version.

Figure 4C and D show the effects of probucol on hERG K^+ currents. Acute bath application of 100 µM probucol affected neither the hERG current amplitude nor the voltage dependence of the activation curve of hERG channels (Fig 4C). The $V_{1/2}$ and slope factor were –5.1 ± 2.3 and 7.2 ± 0.8 mV, respectively, in control. They were –7.2 ± 2.7 and 7.3 ± 0.7 mV in the presence of probucol (n = 5 cells, p>0.05). To test if probucol blocks hERG channels from the internal side of the membrane, we included 100 µM probucol in the pipette solution. We found that the hERG current with 100 µM probucol in the pipette solution was not different from the currents without probucol in the pipette solution (n = 4, data not shown). Thus, probucol does not directly block hERG channels. However, inclusion of probucol in the cell culture medium reduced the hERG current. Figure 4D shows hERG currents from hERG-HEK cells cultured in the control medium (containing 0.3% ethanol vehicle) and in the presence of 30 µM probucol for 48 h. The hERG activation curves under control and probucol-treated conditions are also shown in Fig. 4D. Probucol did not change the voltage dependence of the hERG channel activation ($V_{1/2}$ = –7.5 ± 1.9 mV, k = 6.6 ± 0.2 mV, n = 14 for control; $V_{1/2}$ = –3.4 ± 1.7 mV, k = 7.8 ± 0.4 mV, n = 12 for 30 µM probucol, P>0.05), but significantly reduced the hERG current. To study concentration dependence of probucol effects on hERG current amplitude, tail currents from each probucol-treated cell were normalized to the mean control value (n = 14 cells). The summarized relative tail currents were plotted against probucol concentrations and fitted to Hill equation (n = 9-22 cells at each concentration). The IC_{50} and Hill coefficient were 10.6 µM and 1.0, respectively (Fig. 4D, Bottom).

The chronic nature of probucol-induced hERG and I_{Kr} reduction suggests that probucol may decrease ERG membrane expression. To visualize the surface hERG expression, we performed immunofluorescence staining of cell surface hERG-HAex channels using an anti-HA antibody that

JPET Fast Forward. Published on March 21, 2007 as DOI: 10.1124/jpet.107.120931
This article has not been copyedited and formatted. The final version may differ from this version.

recognizes the HA-epitope located in the extracellular S1-S2 linker of hERG channels. Since we did not permeabilize hERG-HAex-HEK cells, only the extracellularly exposed hERG was stained. As shown in Fig. 5A, the cell surface staining of hERG is visible throughout the control cell. Treatment of hERG-HAex-HEK cells with 100 µM probucol for 48 h significantly reduced the cell surface hERG staining. Figure 5B shows Western blots of hERG proteins extracted from WT hERG-HEK cells cultured in the absence (0.3% ethanol) and presence of 100 µM probucol for 48 h. Probucol essentially eliminated the mature plasma membrane form of hERG channels. Figure 5B right panel shows the densities of the hERG 155 kDa and 135 kDa bands after probucol treatment relative to their respective control values. Probucol treatment reduced the density of the 155 kDa band by 88±7 % ($n = 10$, $p<0.01$), and increased the density of the 135 kDa band by 13±10 % ($n = 10$, $p>0.05$). To confirm the effects of probucol on the surface membrane form of hERG channels, we isolated surface membrane protein using biotinylation method (Cell Surface Protein Isolation Kit, Number 89881, Pierce). The isolated membrane protein from hERG-HEK cells under control conditions (0.3% ethanol) or treated with 100 µM probucol were analyzed using Western blot with anti-hERG antibody (C-20, Santa Cruz; Fig. 5C). Probucol treatment reduced surface membrane hERG by 84 ± 9 % ($n = 4$). To examine the effects of probucol on I_{Kr} expression, Western blots of ERG proteins extracted from neonatal cardiomyocytes cultured in the absence (0.3% ethanol) or presence of 100 µM probucol for 48 h were compared in Fig. 5D. Probucol treatment significantly reduced the 150 and 95 kDa bands, and did not affect the 130 and 85 kDa bands ($n = 4$). Thus, probucol reduced cell surface form of ERG proteins.

To determine the specificity of the probucol-induced hERG/I_{Kr} current reduction, the effects of probucol on Na^+ current (I_{Na}), transient outward K^+ current (I_{to}) and inward rectifier K^+ current (I_{K1})

JPET Fast Forward. Published on March 21, 2007 as DOI: 10.1124/jpet.107.120931
This article has not been copyedited and formatted. The final version may differ from this version.

in neonatal rat cardiomyocytes were examined. Cardiomyocytes were treated with 100 μM probucol for 48 h, and various currents were recorded using specific voltage protocols shown above the corresponding current traces in Fig. 6. The solutions used are summarized in Table 1. Probucol significantly reduced I_{Kr} without affecting I_{Na}, I_{to} or I_{K1}.

Probucol Treatment Prolongs Ventricular Action Potential

The effects of probucol on action potentials recorded in neonatal rat ventricular myocytes were examined. Under control conditions (0.3% ethanol) after 24 h culture, 41% of the cardiomyocytes were quiescent after achieving whole cell configuration (n = 32 cells from 6 isolations, 13 out of 32 cells were quiescent). When 30 μM probucol was added to the cell culture medium, 58% of the ventricular myocytes were quiescent after 24 h culture ($p<0.01$; n = 19 cells from 6 isolations, 11 out of 19 cells were quiescent). Action potentials from the quiescent cells were used for analysis. Consistent with previous reports (Kang *et al.*, 1995; Gaughan *et al.*, 1998), the action potential in control neonatal rat cardiomyocytes displayed a much more pronounced plateau phase than those in adult rat cardiomyocytes (Fig. 7A). Probucol-treatment significantly prolonged action potential duration (Fig. 7B). The action potential durations at 90% repolarization (APD_{90}) under control and probucol-treated conditions are summarized in Fig. 7C. To confirm the role of I_{Kr} in action potential duration, the effect of E-4031, a specific I_{Kr} blocker was examined. The action potentials from neonatal cardiomyocytes in the presence of 100 nM E-4031 were compared with those in control. E-4031 (100 nM) significantly prolonged action potential duration (Fig. 7D-F, n = 12).

JPET Fast Forward. Published on March 21, 2007 as DOI: 10.1124/jpet.107.120931
This article has not been copyedited and formatted. The final version may differ from this version.

DISCUSSION

We identified I_{Kr} in cultured neonatal rat ventricular myocytes. ERG mRNA and protein have been found in the adult rat heart (Wymore *et al.*, 1997; Jones *et al.*, 2004). The existence of I_{Kr} in neonatal rat cardiomyocytes has not been reported. In fact, the systematic electrophysiology data on I_{Kr} in adult rats are lacking possibly due to difficulties in isolating I_{Kr} from other coexisting K^+ currents such as I_{to}. We have found that Cs^+ uniquely permeates hERG and we have used Cs^+ permeation in successfully isolating I_{Kr} in rabbit ventricular myocytes (Zhang, 2006). The clone of rat ERG is 96% identical to hERG at the amino acid level (Wymore *et al.*, 1997). In the present study, we have recorded robust Cs^+-carried I_{Kr} in neonatal rat ventricular myocytes. Since Cs^+ slows hERG/I_{Kr} inactivation (Zhang, 2006), there are differences in current kinetics between K^+-carried and Cs^+-carried I_{Kr} (Zhang, 2006). As well, the IC_{50} for E-4031 to block Cs^+-carried I_{Kr} is higher than that to block K^+-carried I_{Kr} (Fig. 1 and Fig. 2) (Zhang, 2006). Despite these differences, the Cs^+-carried I_{Kr} recording represents a simple and reliable way to study I_{Kr} density, and greatly facilitates studies of drug-induced alterations of I_{Kr} expression. Presently, models for studying native I_{Kr} trafficking at the protein level are not available. hERG turnover time is about 11 h in hERG-HEK cells (Ficker *et al.*, 2003), and I_{Kr} turnover time in adult cardiomyocytes is likely to be much slower. Since neonatal cardiomycytes have a more vigorous metabolism than adult cardiomyocytes, identification of I_{Kr} in neonatal cardiomyocyte provides us with a very useful way to analyze the native I_{Kr} trafficking. Significantly, using this model, we discovered that probucol reduces functional I_{Kr} expression. Previously, pentamidine was reported to disrupt hERG trafficking and cause LQTS (Kuryshev *et al.*, 2005; Cordes *et al.*, 2005). We found that like probucol, pentamidine treatment (10 μM, 48 h) significantly reduced the 150 and 95 kDa bands, and did not affect the 130 and 85 kDa bands of ERG of neonatal rat cardiomyocytes (n = 4, data not shown).

JPET Fast Forward. Published on March 21, 2007 as DOI: 10.1124/jpet.107.120931
This article has not been copyedited and formatted. The final version may differ from this version.

Probucol is a cholesterol-lowering drug that has been found to cause long QT syndrome and Torsades de Pointes arrhythmia in patients, and sudden cardiac death in experimental animals (Elharrar *et al.*, 1979; McCaughan, 1982; Dujovne *et al.*, 1984; Browne *et al.*, 1984; Matsuhashi *et al.*, 1989; Tamura *et al.*, 1994; Reinoehl *et al.*, 1996; Hayashi *et al.*, 2004). Our data indicate that chronic probucol exposure reduces the hERG current with an IC_{50} of 10.6 µM, and reduces native I_{Kr} with an IC_{50} of 20.6 µM. We chose 48 h treatment of cells with probucol because the turnover of the hERG channel occurs at a rather slow rate (approximately 11 hours) (Ficker *et al.*, 2003). The recommended daily dosage of probucol for human adults is 1 g. In one reported probucol-induced LQTS and Torsades de Pointes arrhythmia case, the serum probucol concentration measured during the cardiac arrhythmia was 26 µg/ml (Hayashi *et al.*, 2004), which is equivalent to 50.3 µM. In patients who received probucol 1 g daily for periods of 1 to 12 months, the mean plasma levels ranged from 18.2 to 39.2 µg /ml (35.2 – 75.9 µM) (Heeg and Tachizawa, 1980). Although the drug concentrations that reach cardiac myocytes are unknown, it seems that clinically relevant concentrations of probucol are able to cause I_{Kr} reduction and LQTS.

About 200 LQT2-associated hERG mutations have been identified in humans, and missense (single amino acid substitution) mutations represent the dominant predicted protein abnormality (Anderson *et al.*, 2006). While some patients with hERG mutations may have a prolonged QT interval and clinically be asymptomatic, they are likely more vulnerable to drugs that interact with hERG channels. Previously, Hayashi *et al.* reported that hERG M124T mutation caused a mild-to-moderate channel dysfunction but manifested marked QT prolongation or Torsade de Pointes after taking probucol (Hayashi *et al.*, 2004). They demonstrated that probucol acts to alter hERG function due to a ~10 mV depolarization shift of activation curve (Hayashi *et al.*, 2004). The

JPET Fast Forward. Published on March 21, 2007 as DOI: 10.1124/jpet.107.120931
This article has not been copyedited and formatted. The final version may differ from this version.

authors also reported that acutely applied probucol shifted the reversal potential of hERG channels (Hayashi *et al.*, 2004). Our data obtained in hERG-HEK cells and in neonatal rat ventricular myocytes showed that probucol has no acute effect on either hERG or I_{Kr} currents. The reason for the discrepancy between our data and those of Hayashi *et al.* is unknown. The study reported by Hayashi *et al.* was performed in Xenopus oocytes. However, usually higher concentrations of drugs are needed to block channels expressed in Xenopus oocytes compared with those needed in mammalian cells. There has been no other evidence showing that probucol blocks hERG channels. On the other hand, our finding that probucol disrupts I_{Kr}/hERG cell membrane expression provides a plausible explanation for probucol-induced LQTS and Torsade de Pointes.

hERG proteins are synthesized in the Endoplasmic Reticulum (ER) and transported to the cell surface via the Golgi apparatus. Misfolded or misassembled proteins are retained in the ER by its quality control mechanism. It is thought that mutations can cause misfolding of hERG proteins, resulting in trafficking defect (Anderson *et al.*, 2006). Since probucol treatment did not reduce the intracellular forms of ERG (135 kDa band of hERG, 130 and 85 kDa bands of ERG in cardiomyocytes, Fig. 5), the probucol-induced ERG membrane expression does not seem to be a result of inhibition of the channel synthesis. Instead, it could develop from either defective trafficking or accelerated membrane ERG degradation. It has been shown that E-4031, glycerol or culture in low temperature can rescue some forms of trafficking deficient mutant hERG channels (Zhou *et al.*, 1999). However, we found that none of these manipulations rescued probucol-disrupted hERG surface expression (data not shown). Probucol is a very lipophilic drug that can inhibit the cholesterol synthesis in the cell and may modify the lipid content of the membrane. Whether the lipid content of the cell contributes to hERG/I_{Kr} functional expression needs further investigation.

JPET Fast Forward. Published on March 21, 2007 as DOI: 10.1124/jpet.107.120931
This article has not been copyedited and formatted. The final version may differ from this version.

In summary, the present study provides evidence that probucol does not block hERG or I_{Kr} channels but disrupts ERG protein trafficking. In drug development, early screening of lead compounds for potential acute hERG channel blockade is becoming a common practice. The finding that probucol reduces hERG and I_{Kr} currents by reducing the number of functional ERG channels suggests that further strategies for evaluating the LQTS-risk of drugs should be considered.

JPET Fast Forward. Published on March 21, 2007 as DOI: 10.1124/jpet.107.120931
This article has not been copyedited and formatted. The final version may differ from this version.

Acknowledgements

We thank Dr. Craig January (University of Wisconsin) for providing the hERG expressing stable cell line; Dr. Gail Robertson (University of Wisconsin) for the hERG cDNA. We thank Dr. Xie's and Dr. Dhalla's labs (University of Manitoba) for technical advice. We thank Drs. Jeffrey Wigle, Jiuyong Xie and Nasrin Mesaeli for helpful discussion.

JPET Fast Forward. Published on March 21, 2007 as DOI: 10.1124/jpet.107.120931
This article has not been copyedited and formatted. The final version may differ from this version.

References

Abbott GW, Sesti F, Splawski I, Buck ME, Lehmann WH, Timothy KW, Keating MT, and Goldstein SAN (1999) MiRP1 forms I_{Kr} potassium channels with HERG and is associated with cardiac arrhythmia. *Cell* **97**:175-187.

Anderson CL, Delisle BP, Anson BD, Kilby JA, Will ML, Tester DJ, Gong Q, Zhou Z, Ackerman MJ, and January CT (2006) Most LQT2 mutations reduce Kv11.1 (hERG) current by a class 2 (trafficking-deficient) mechanism. *Circulation* **113**:365-373.

Baetz D, Regula KM, Ens K, Shaw J, Kothari S, Yurkova N, and Kirshenbaum LA (2005) Nuclear factor-kappaB-mediated cell survival involves transcriptional silencing of the mitochondrial death gene BNIP3 in ventricular myocytes. *Circulation* **112**:3777-3785.

Browne KF, Prystowsky EN, Heger JJ, Cerimele BJ, Fineberg N, and Zipes DP (1984) Prolongation of the QT interval induced by probucol: demonstration of a method for determining QT interval change induced by a drug. *Am Heart J* **107**:680-684.

Cordes JS, Sun Z, Lloyd DB, Bradley JA, Opsahl AC, Tengowski MW, Chen X, and Zhou J (2005) Pentamidine reduces hERG expression to prolong the QT interval. *Br J Pharmacol* **145**:15-23.

Dujovne CA, Atkins F, Wong B, DeCoursey S, Krehbiel P, and Chernoff SB (1984) Electrocardiographic effects of probucol. A controlled prospective clinical trial. *Eur J Clin Pharmacol* **26**:735-739.

Elharrar V, Watanabe AM, Molello J, Besch HR, Jr., and Zipes DP (1979) Adrenergaically mediated ventricular fibrillation in probucol-treated dogs: roles of alpha and beta adrenergic receptors. *Pacing Clin Electrophysiol* **2**:435-443.

JPET Fast Forward. Published on March 21, 2007 as DOI: 10.1124/jpet.107.120931
This article has not been copyedited and formatted. The final version may differ from this version.

Ficker E, Dennis AT, Wang L, and Brown AM (2003) Role of the cytosolic chaperones Hsp70 and Hsp90 in maturation of the cardiac potassium channel HERG. *Circ Res* **92**:e87-100.

Ficker E, Kuryshev YA, Dennis AT, Obejero-Paz C, Wang L, Hawryluk P, Wible BA, and Brown AM (2004) Mechanisms of arsenic-induced prolongation of cardiac repolarization. *Mol Pharmacol* **66**:33-44.

Gaughan JP, Hefner CA, and Houser SR (1998) Electrophysiological properties of neonatal rat ventricular myocytes with α_1-adrenergic-induced hypertrophy. *Am J Physiol Heart Circ Physiol* **275**:H577-H590.

Gong J, Xu J, Bezanilla M, Van Huizen R, Derin R, and Li M (1999) Differential stimulation of PKC phosphorylation of potassium channels by ZIP1 and ZIP2. *Science* **285**:1565-1569.

Hamill OP, Marty A, Neher E, Sakmann B, and Sigworth FJ (1981) Improved patch-clamp techniques for high-resolution current recording from cells and cell-free membrane patches. *Pflugers Arch* **391**:85-100.

Hayashi K, Shimizu M, Ino H, Yamaguchi M, Terai H, Hoshi N, Higashida H, Terashima N, Uno Y, Kanaya H, and Mabuchi H (2004) Probucol aggravates long QT syndrome associated with a novel missense mutation M124T in the N-terminus of HERG. *Clin Sci (Lond)* **107**:175-182.

Heeg JF and Tachizawa H (1980) Plasma levels of probucol in man after single and repeated oral doses (author's transl). *Nouv Presse Med* **9**:2990-2994.

Jones DB, Simpson HC, Slaughter P, Lousley S, Carter RD, Cobbe SM, and Mann JI (1984) A comparison of cholestyramine and probucol in the treatment of familial hypercholesterolaemia. *Atherosclerosis* **53**:1-7.

JPET Fast Forward. Published on March 21, 2007 as DOI: 10.1124/jpet.107.120931
This article has not been copyedited and formatted. The final version may differ from this version.

Jones EM, Roti Roti EC, Wang J, Delfosse SA, and Robertson GA (2004) Cardiac IKr channels minimally comprise hERG1a and 1b subunits. *J Biol Chem*.

Kang JX, Xiao YF, and Leaf A (1995) Free, long-chain, polyunsaturated fatty acids reduce membrane electrical excitability in neonatal rat cardiac myocytes. *Proc Natl Acad Sci U S A* **92**:3997-4001.

Keating MT and Sanguinetti MC (2001) Molecular and cellular mechanisms of cardiac arrhythmias. *Cell* **104**:569-580.

Kuryshev YA, Ficker E, Wang L, Hawryluk P, Dennis AT, Wible BA, Brown AM, Kang J, Chen XL, Sawamura K, Reynolds W, and Rampe D (2005) Pentamidine-induced long QT syndrome and block of hERG trafficking. *J Pharmacol Exp Ther* **312**:316-323.

Matsuhashi H, Onodera S, Kawamura Y, Hasebe N, Kohmura C, Yamashita H, and Tobise K (1989) Probucol-induced QT prolongation and torsades de pointes. *Jpn J Med* **28**:612-615.

McCaughan D (1982) Probucol and the QT interval. *Lancet* **2**:161.

Rajamani S, Eckhardt LL, Valdivia CR, Klemens CA, Gillman BM, Anderson CL, Holzem KM, Delisle BP, Anson BD, Makielski JC, and January CT (2006) Drug-induced long QT syndrome: hERG K+ channel block and disruption of protein trafficking by fluoxetine and norfluoxetine. *Br J Pharmacol* **149**:481-489.

Reinoehl J, Frankovich D, Machado C, Kawasaki R, Baga JJ, Pires LA, Steinman RT, Fromm BS, and Lehmann MH (1996) Probucol-associated tachyarrhythmic events and QT prolongation: importance of gender. *Am Heart J* **131**:1184-1191.

JPET Fast Forward. Published on March 21, 2007 as DOI: 10.1124/jpet.107.120931
This article has not been copyedited and formatted. The final version may differ from this version.

Sanguinetti MC, Jiang C, Curran ME, and Keating MT (1995) A mechanistic link between an inherited and an acquired cardiac arrhythmia: *HERG* encodes the I_{Kr} potassium channel. *Cell* **81**:299-307.

Sanguinetti MC and Tristani-Firouzi M (2006) hERG potassium channels and cardiac arrhythmia. *Nature* **440**:463-469.

Tamura M, Ueki Y, Ohtsuka E, Oribe M, Seita M, Oribe K, and Ito M (1994) Probucol-induced QT prolongation and syncope. *Jpn Circ J* **58**:374-377.

Trudeau MC, Warmke JW, Ganetzky B, and Robertson GA (1995) HERG, a human inward rectifier in the voltage-gated potassium channel family. *Science* **269**:92-95.

Wymore RS, Gintant GA, Wymore RT, Dixon JE, McKinnon D, and Cohen IS (1997) Tissue and species distribution of mRNA for the IKr-like K^+ channel, erg. *Circ Res* **80**:261-268.

Zhang S (2006) Isolation and characterization of IKr in cardiac myocytes by Cs+ permeation. *Am J Physiol Heart Circ Physiol* **290**:H1038-H1049.

Zhou Z, Gong Q, Epstein ML, and January CT (1998a) HERG channel dysfunction in human long QT syndrome. Intracellular transport and functional defects. *J Biol Chem* **273**:21061-21066.

Zhou Z, Gong Q, and January CT (1999) Correction of defective protein trafficking of a mutant HERG potassium channel in human long QT syndrome. Pharmacological and temperature effects. *J Biol Chem* **274**:31123-31126.

JPET Fast Forward. Published on March 21, 2007 as DOI: 10.1124/jpet.107.120931
This article has not been copyedited and formatted. The final version may differ from this version.

Zhou Z, Gong Q, Ye B, Fan Z, Makielski JC, Robertson GA, and January CT (1998b) Properties of HERG channels stably expressed in HEK 293 cells studied at physiological temperature. *Biophys J* **74**:230-241.

JPET Fast Forward. Published on March 21, 2007 as DOI: 10.1124/jpet.107.120931
This article has not been copyedited and formatted. The final version may differ from this version.

Footnotes

The project was supported by operating grants from the Canadian Institutes of Health Research and the Heart and Stroke Foundation of Manitoba to Shetuan Zhang, who is a recipient of the New Investigator Award from the Heart and Stroke Foundation of Canada.

Legends for Figures

Fig. 1. K^+- and Cs^+-carried I_{Kr} in neonatal rat ventricular myocytes. A, families of K^+ currents in control conditions (a), in the presence of 1 μM E-4031 (b), and the E-4031 sensitive currents (c). B, the I-V relationship and the activation curve of the E-4031 sensitive current. The currents at the end of depolarizing steps were measured for I-V relationship and the peak tail currents were measured for activation curve (n = 4). C, families of the Cs^+ currents. D, I-V relationships of the maximal currents during depolarizations (▲) and the currents at the end of depolarizing steps (■, n = 8). E, activation curve of the Cs^+ tail current (●, n = 8).

Fig. 2. Properties of the I_{Kr} Cs^+ current in neonatal rat ventricular myocytes. A, the voltage-dependent inactivation. B, the voltage-dependent recovery from inactivation and deactivation. C, summarized voltage dependences of τ_{rec} (▲) and τ_{inact} (▼). D and E, the voltage-dependent inactivation of the Cs^+ current (Cs^+_i: 135 mM) in 0 (D) and 135 mM Cs^+_o (E). Elevation of Cs^+_o slowed the current inactivation. F, the τ_{inact}–voltage relationships of the Cs^+ current in the absence (▽) and presence of 135 mM Cs^+_o (▼, n = 4 cells). G and H, families of Cs^+ currents in the absence and presence of 3 μM E-4031. I, concentration-dependent block of Cs^+ current by E-4031. Tail currents at –80 mV following a depolarization to +50 mV were plotted against drug concentrations and fitted to the Hill equation.

Fig. 3. Effects of hERG siRNA transfection on I_{Kr} and hERG expression. A, ERG expression in neonatal rat ventricular myocytes in control (Ctrl) and after proteinase K treatment (PK, n = 5). B, hERG expression in control hERG-HEK cells (Ctrl) and after proteinase K treatment (PK, n = 3). C,

JPET Fast Forward. Published on March 21, 2007 as DOI: 10.1124/jpet.107.120931
This article has not been copyedited and formatted. The final version may differ from this version.

ERG expression in cultured neonatal rat ventricular myocytes transfected with control siRNA or hERG siRNA (n = 4). D, hERG expression in hERG-HEK cells transfected with control siRNA or hERG siRNA (n = 3). E, families of Cs^+ currents in neonatal rat ventricular myocytes transfected with control siRNA (n = 10) or hERG siRNA (n = 16). The voltage protocol shown in Fig. 1C was used. F, families of hERG K^+ currents in hERG-HEK cells transfected with control siRNA (n = 8) or hERG siRNA (n = 9). For hERG K^+ current recordings, the cells were held at –80 mV and depolarized to voltages between –70 and 70 mV for 4 s. The depolarizing steps were followed by a repolarization to –50 mV to record tail currents (see Fig. 4C).

Fig. 4. Chronic probucol treatment reduces I_{Kr} in cultured neonatal rat cardiomyocytes and the recombinant hERG current. A, acute effects of probucol on the I_{Kr} Cs^+ current. B, chronic effects of probucol on the I_{Kr} Cs^+ currents. The Cs^+ tail currents at –80 mV following various activation voltages in absence (○) and presence of probucol (●) are shown under current traces. Concentration-dependent effect of chronic probucol treatment on Cs^+-carried I_{Kr} tail current amplitudes in neonatal cardiac myocytes is shown at the bottom of panel B. C and D, families of K^+-carried hERG currents in the absence and presence of acute (C) or chronic (D) probucol application. Activation curves of K^+-carried hERG currents in the absence (○) and presence of probucol (●) are shown under the current traces. Concentration-dependent reduction of K^+-carried hERG tail current amplitudes by chronic (48 h) probucol exposure is shown at the bottom of panel D.

Fig. 5. Probucol reduces membrane ERG protein expression. A, non-permeabilized hERG-HEK cells in control (left) and after 48 h treatment with 100 μM probucol (right) were immunofluorescently stained using a primary anti-HA antibody and a green fluorescent conjugated

secondary antibody. For each lane, the upper photo shows the immunofluorescent image and the lower photo shows the phase contrast image of the same cell. B, Western blots showing the effect of probucol on hERG expression. Equal loading of proteins were ensured by monitoring actin density. The right panel shows the summarized relative densities of hERG 155 kDa and 135 kDa bands from probucol-treated (100 μM, 48 h) hERG-HEK cells to the corresponding densities from control cells. C, Western blots showing the effect of probucol on biotinylation isolated surface membrane protein. hERG protein was detected with gaot anti-hERG primary antibody (Stan Cruz) and donkey anti-goat secondary antibody (Invitrogen). Rabbit anti-pan Cadherin primary antibody and mouse anti-rabbit secondary were used to detect pan Cadherin (135 kDa) which was used as a control for biotinylated cell surface protein. D, Western blots showing the effect of probucol on I_{Kr} expression in neonatal rat ventricular myocytes. The control lane shows four molecular bands of ERG proteins at approximately 150, 130, 95 and 85 kDa. Probucol treatment significantly reduced the 150 and 95 kDa bands. Right panel shows the summarized relative densities of each band of I_{Kr} from probucol-treated (100 μM, 48 h) myocytes to the corresponding densities from control cells. ** indicates $p<0.01$.

Fig. 6. Probucol reduces I_{Kr} without affecting I_{Na}, I_{to} or I_{K1} in neonatal rat cardiomyocytes. The upper and middle panels show the families of the I_{Kr}, I_{Na}, I_{K1} and I_{to} currents in control and probucol-treated (100 μM, 48 h) cardiomyocytes. The lower panels show the summarized I-V relationships of the I_{Kr} tail current (n = 12 for probucol treated, n = 9 for control), I_{Na} (n = 7 for probucol treated, n = 6 for control), I_{K1} (n = 6 for probucol treated, n = 7 for control, currents were measured at the end of 1 s pulses) and I_{to} peak currents (n = 3 for probucol treated, n = 4 for control).

JPET Fast Forward. Published on March 21, 2007 as DOI: 10.1124/jpet.107.120931
This article has not been copyedited and formatted. The final version may differ from this version.

Fig. 7. Probucol prolongs the action potential duration in rat neonatal cardiomyocytes. A, action potential from a control cardiomyocyte. B, action potential from a probucol-treated cardiomyocyte (30 μM, 24 h). C, summarized action potential duration in control and probucol-treated cardiomyocytes. D and E, action potentials from cardiomyocytes in the absence (D) and presence of 100 nM E-4031 (E). F, summarized action potential duration in the absence and presence of 100 nM E-4031. Action potentials were elicited by injecting currents of 1 ms duration with amplitude 1.2 times the threshold through the recording electrode. ** indicates $p<0.01$.

JPET Fast Forward. Published on March 21, 2007 as DOI: 10.1124/jpet.107.120931
This article has not been copyedited and formatted. The final version may differ from this version.

Table 1: Compositions of solutions for recording various currents (in mM). The pH of the bath solutions was 7.4, and the pH of the pipette solutions was 7.2, adjusted using appropriate hydroxide salts or HCl.

I_{hERG}, $I_{Kr\text{-}K}$	Bath:	5 KCl, 130 NaCl, 1 $MgCl_2$, 2 $CaCl_2$, 10 glucose,10 HEPES
	Pipette:	135 KCl, 10 EGTA, 1 $MgCl_2$, 10 HEPES
$I_{Kr\text{-}Cs}$	Bath:	135 CsCl, 1 $MgCl_2$, 10 glucose, 10 HEPES, 10 µM Nifedipine
	Pipette:	135 CsCl, 10 EGTA, 5 MgATP, 10 HEPES
I_{Na}	Bath:	100 TEACl, 40 NaCl, 5 KCl, 1 MgCl, 2 $CaCl_2$, 10 glucose, 10 HEPES
	Pipette:	135 CsCl, 10 EGTA, 5 MgATP, 10 HEPES
I_{K1}, I_{to}*	Bath:	5.4 KCl, 130 NMDG, 1 $MgCl_2$, 2 $CaCl_2$, 10 glucose, 10 HEPES, 1 µM Nifedipine
	Pipette:	135 KCl, 10 EGTA, 1 $MgCl_2$, 5 MgATP, 10 HEPES
AP	Bath:	5 KCl, 130 NaCl, 1 $MgCl_2$, 2 $CaCl_2$, 10 glucose, 10 HEPES
	Pipette:	135 KCl, 10 EGTA, 1 $MgCl_2$, 5 MgATP, 10 HEPES

* I_{to} was obtained using current subtraction method with I_{to} blocker 4-AP (10 mM).

Figure 1

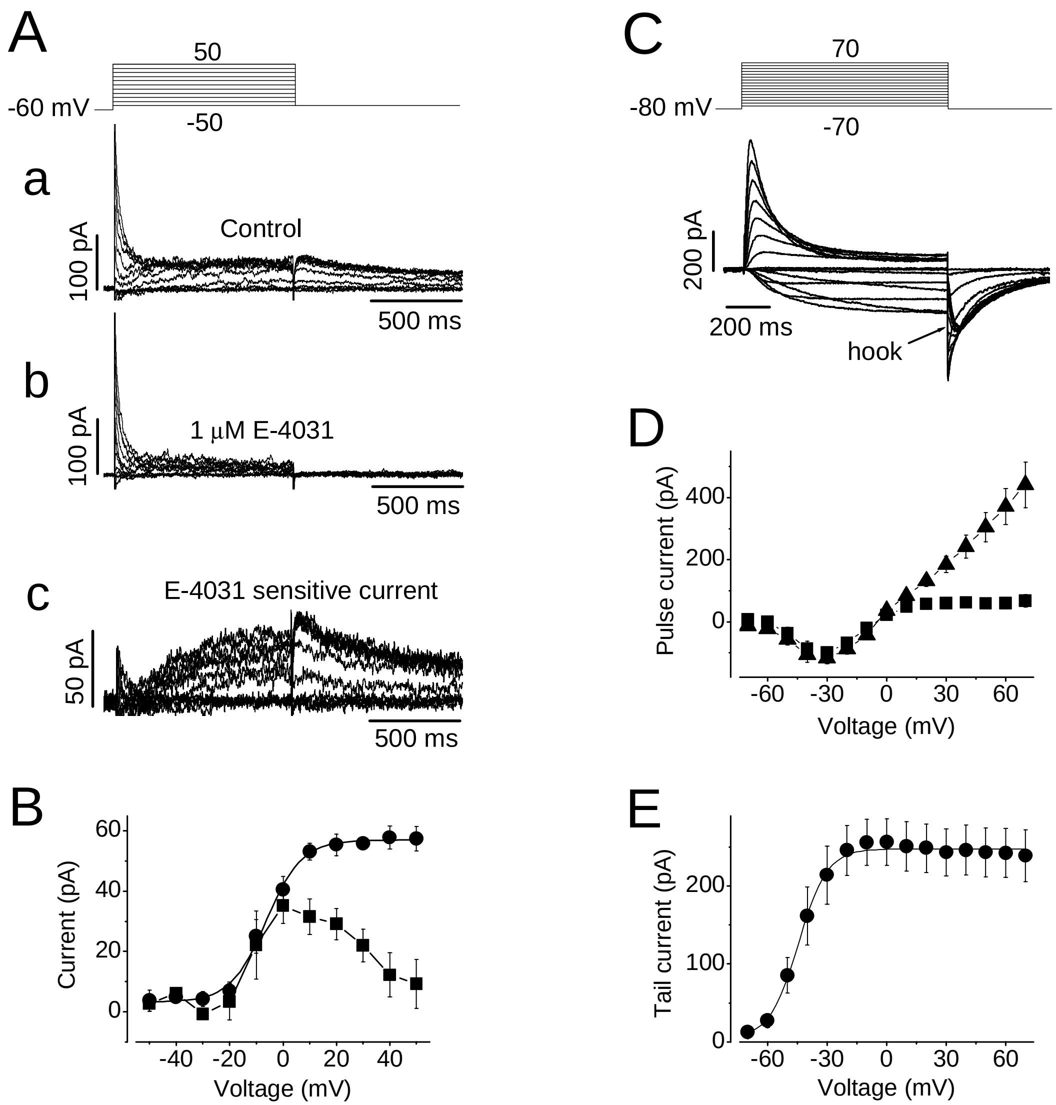

A
50
-60 mV
-50
a
Control
100 pA
500 ms
b
1 µM E-4031
100 pA
500 ms
c
E-4031 sensitive current
50 pA
500 ms
B
Current (pA)
60
40
20
0
-40
-20
0
20
40
Voltage (mV)
C
70
-80 mV
-70
200 pA
200 ms
hook
D
Pulse current (pA)
400
200
0
-60
-30
0
30
60
Voltage (mV)
E
Tail current (pA)
200
100
0
-60
-30
0
30
60
Voltage (mV)

Figure 2

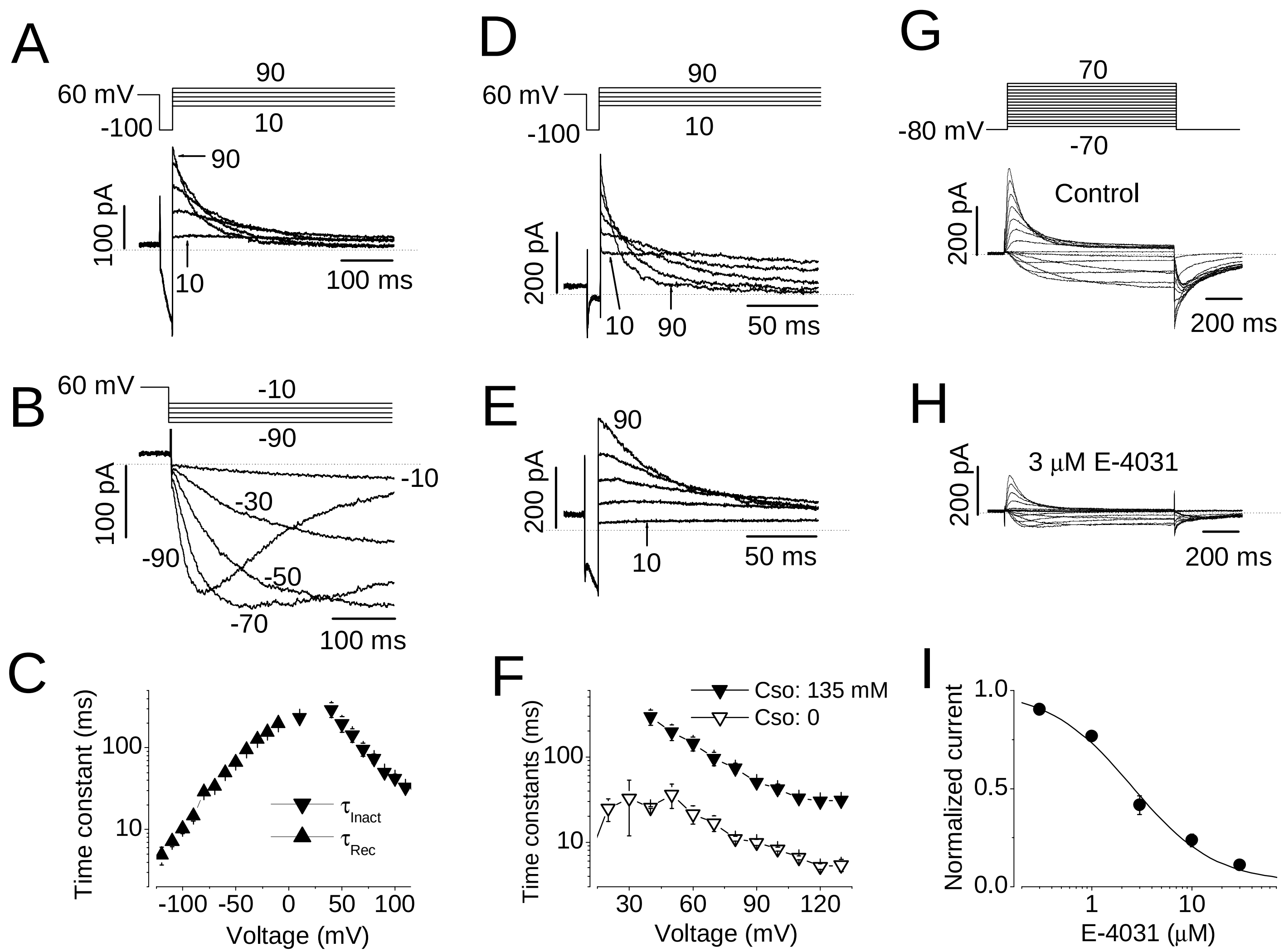

A
60 mV
-100
90
10
100 pA
100 ms
B
60 mV
-10
-90
-30
-50
-70
100 pA
100 ms
C
Time constant (ms)
Voltage (mV)
τInact
τRec
D
60 mV
-100
90
10
200 pA
50 ms
E
200 pA
50 ms
F
Cso: 135 mM
Cso: 0
Time constants (ms)
Voltage (mV)
G
70
-80 mV
-70
Control
200 pA
200 ms
H
3 μM E-4031
200 pA
200 ms
I
Normalized current
E-4031 (μM)

Figure 3

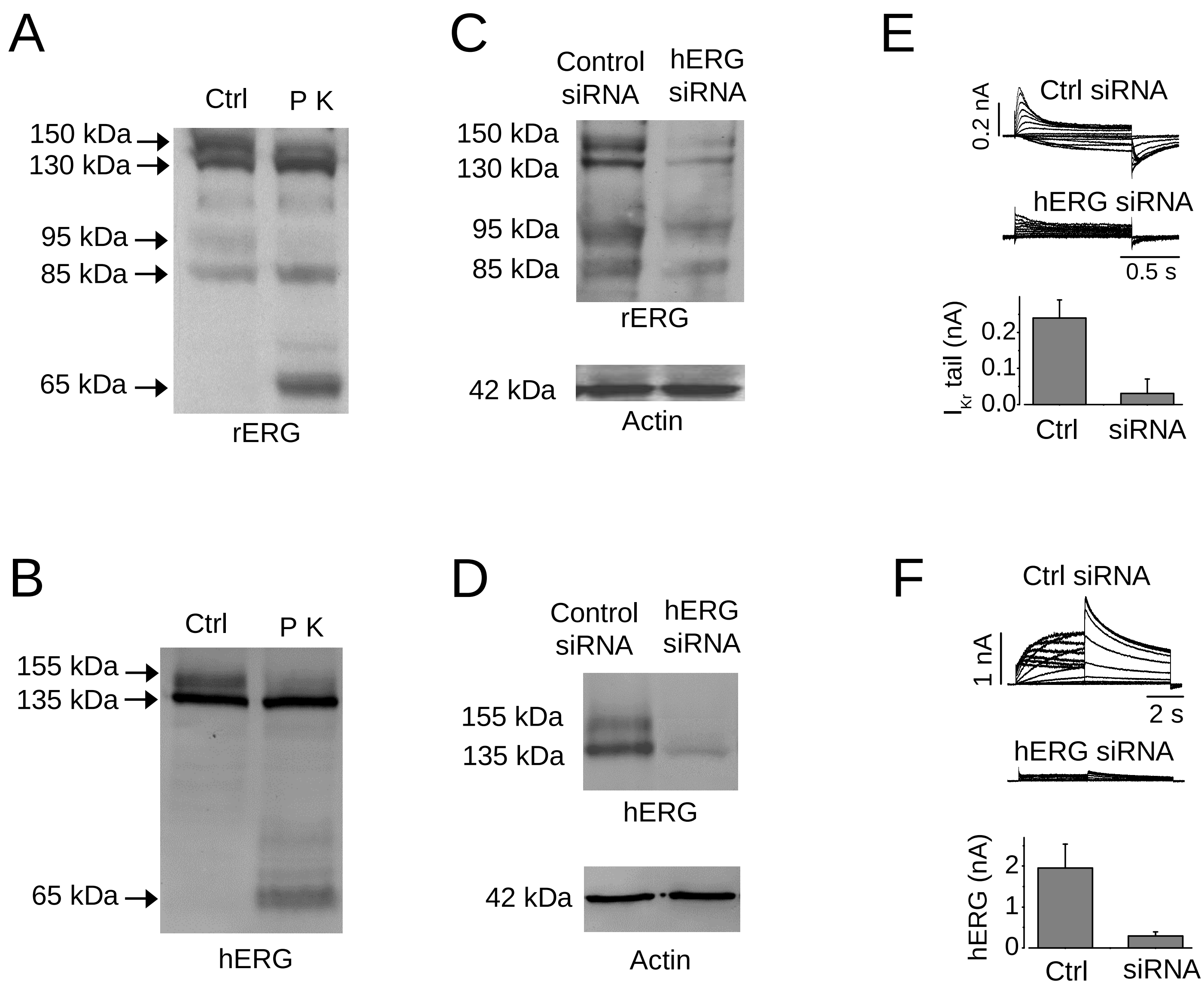

JPET Fast Forward. Published on March 21, 2007 as DOI: 10.1124/jpet.107.120931
This article has not been copyedited and formatted. The final version may differ from this version.

Figure 4

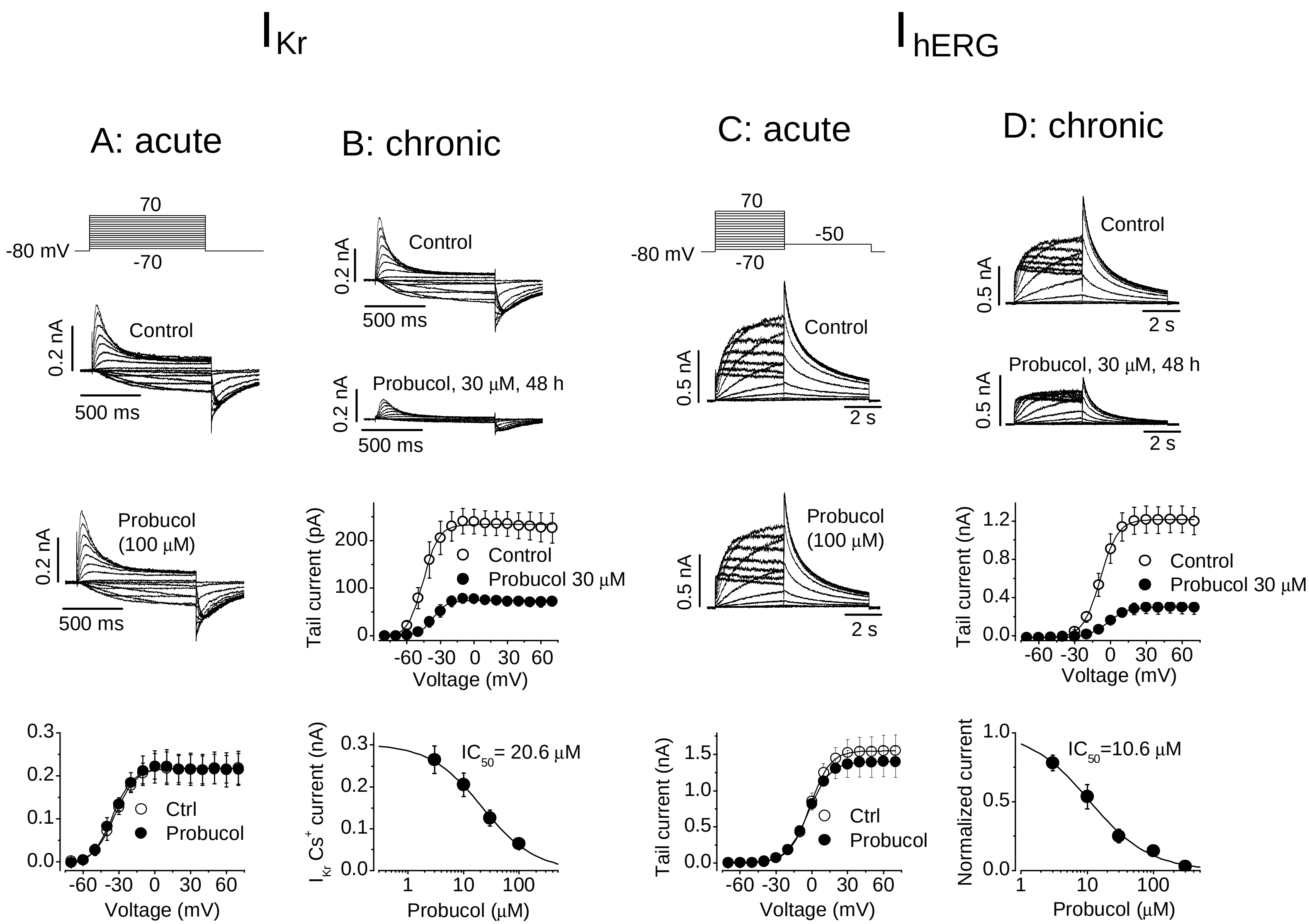

I Kr
I hERG
A: acute
B: chronic
C: acute
D: chronic
70
-80 mV
-70
-50
Control
Probucol (100 µM)
Probucol, 30 µM, 48 h
0.2 nA
0.5 nA
500 ms
2 s
Tail current (pA)
Tail current (nA)
Voltage (mV)
Control
Probucol 30 µM
Ctrl
Probucol
IKr Cs+ current (nA)
IC50= 20.6 µM
IC50=10.6 µM
Normalized current
Probucol (µM)

Figure 5

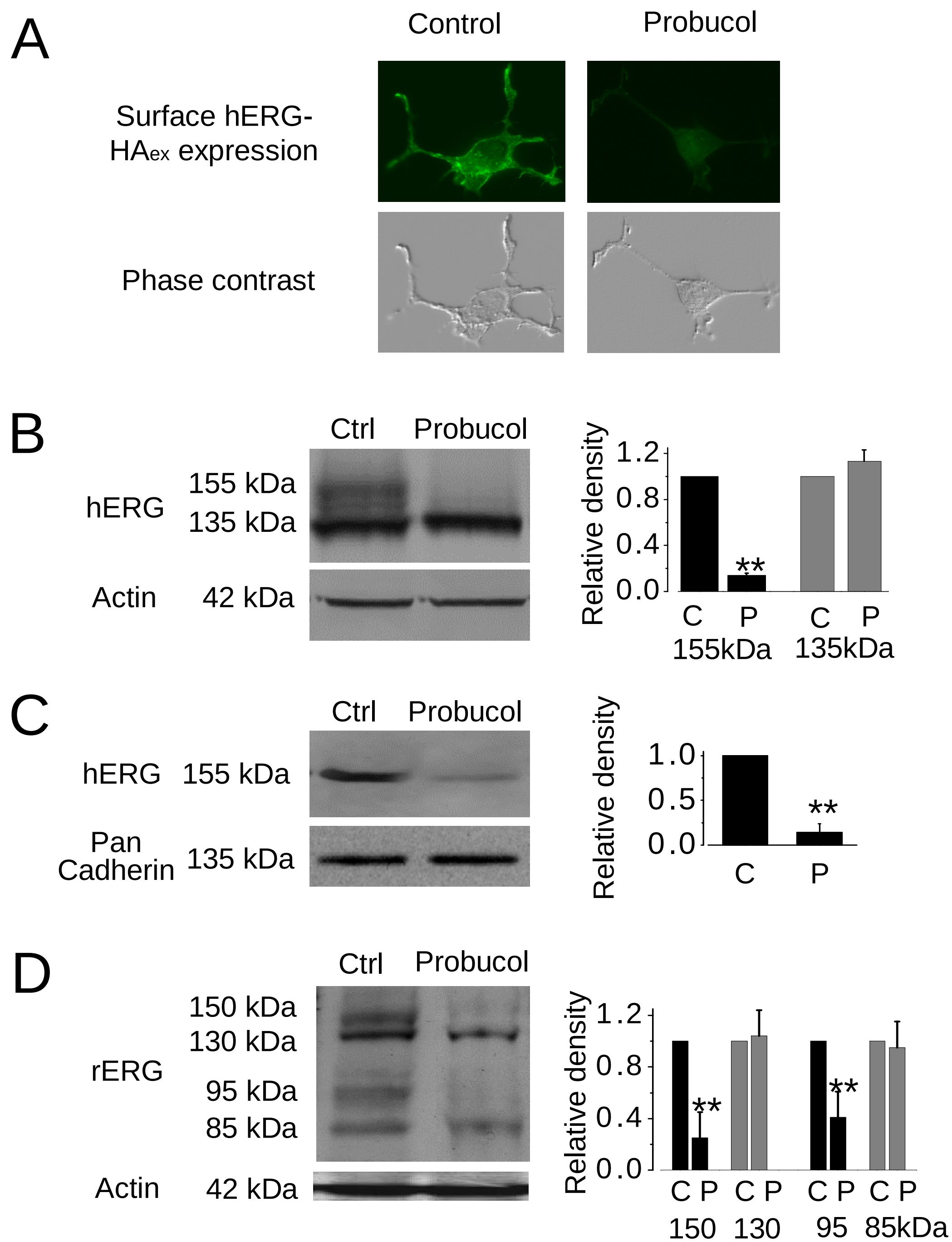
A
Control
Probucol
Surface hERG-HAex expression
Phase contrast
B
Ctrl
Probucol
hERG
155 kDa
135 kDa
Actin
42 kDa
Relative density
1.2
0.8
0.4
0.0
**
C P
155kDa
C P
135kDa
C
Ctrl
Probucol
hERG
155 kDa
Pan Cadherin
135 kDa
Relative density
1.0
0.5
0.0
**
C
P
D
Ctrl
Probucol
rERG
150 kDa
130 kDa
95 kDa
85 kDa
Actin
42 kDa
Relative density
1.2
0.8
0.4
0.0
**
**
C P C P C P C P
150 130 95 85kDa

Figure 6

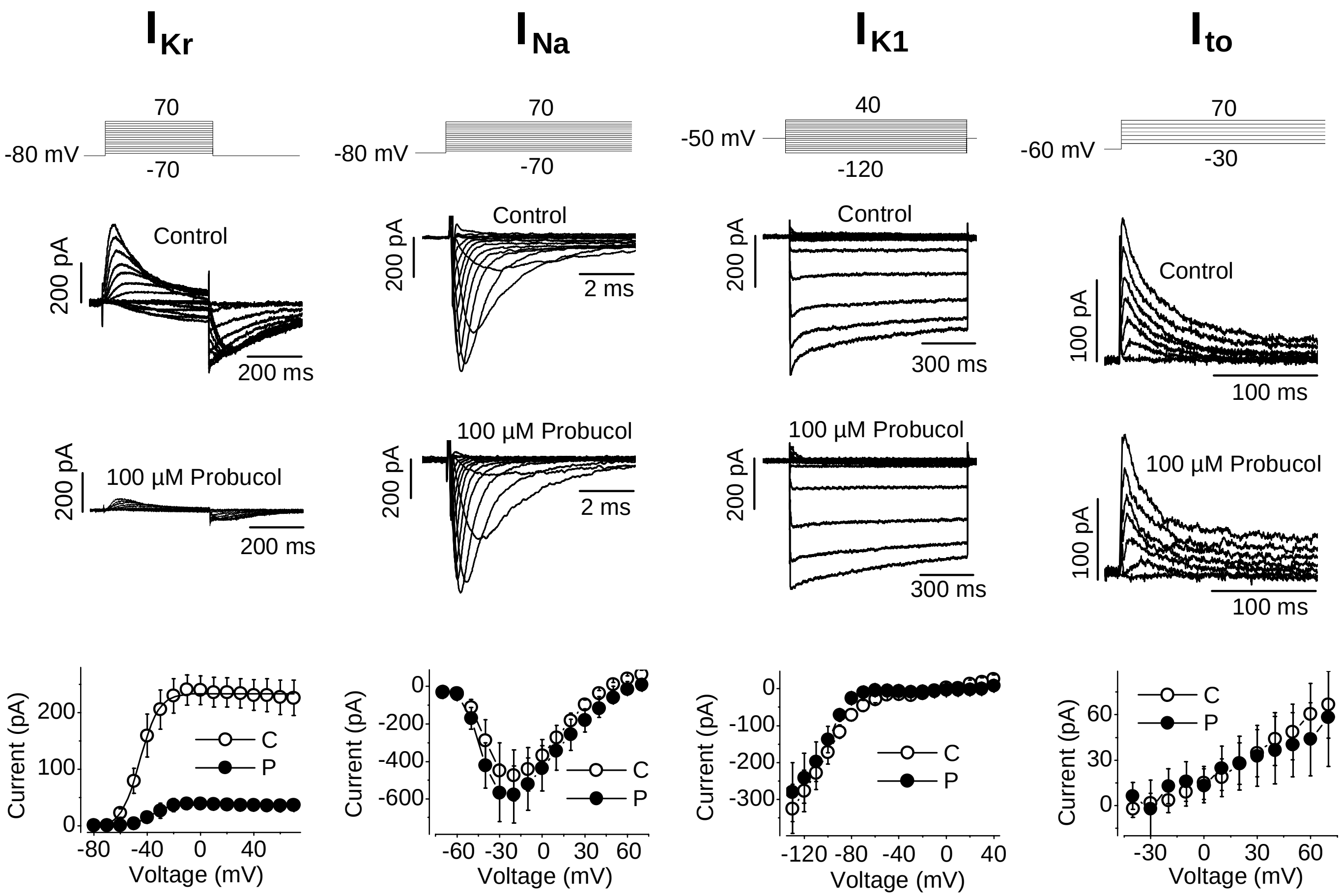

I_{Kr}
I_{Na}
I_{K1}
I_{to}
70
-80 mV
-70
70
-80 mV
-70
40
-50 mV
-120
70
-60 mV
-30
Control
200 pA
200 ms
Control
200 pA
2 ms
Control
200 pA
300 ms
Control
100 pA
100 ms
100 µM Probucol
200 pA
200 ms
100 µM Probucol
200 pA
2 ms
100 µM Probucol
200 pA
300 ms
100 µM Probucol
100 pA
100 ms
Current (pA)
Voltage (mV)
C
P

Figure 7

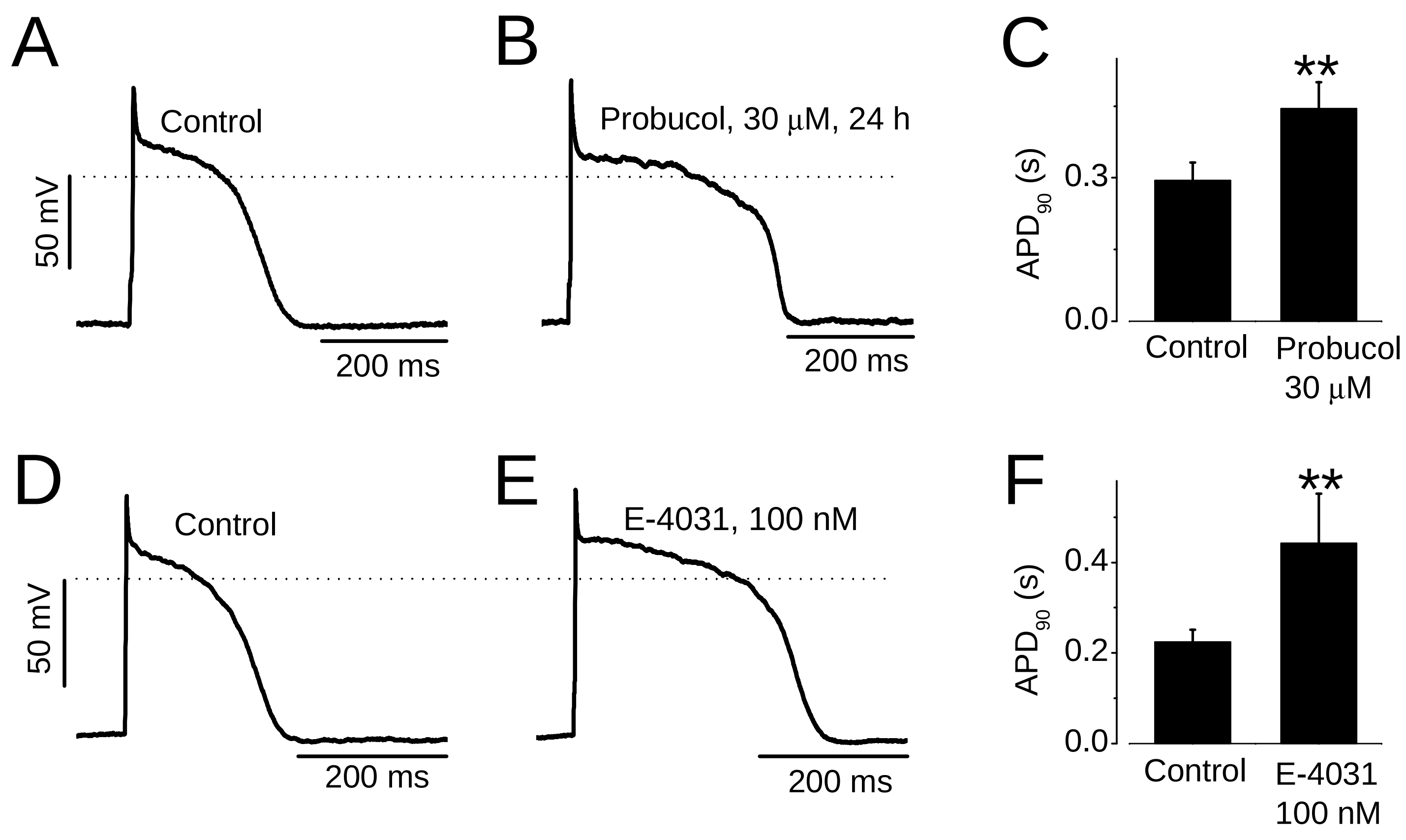
A
Control
50 mV
200 ms
B
Probucol, 30 μM, 24 h
200 ms
C
**
APD90 (s)
0.3
0.0
Control
Probucol
30 μM
D
Control
50 mV
200 ms
E
E-4031, 100 nM
200 ms
F
**
APD90 (s)
0.4
0.2
0.0
Control
E-4031
100 nM